Usui and Yamazaki
Progress in Earth and Planetary Science (2023) 10:47
https://doi.org/10.1186/s40645-023-00581-z

Progress in Earth and Planetary Science

RESEARCH ARTICLE Open Access

K-feldspar enrichment in the Pacific pelagic sediments before Miocene

Yoichi Usui[1,2*] and Toshitsugu Yamazaki[3]

Abstract

The mineralogy of atmospheric silicate dust controls its interaction with clouds. K-feldspar has a remarkably high ice-nucleating activity, and its distribution may have influenced the global climate throughout Earth's history. However, long-term archives of past atmospheric feldspar are not known. Here, we investigate feldspar mineralogy, content, and grain size in pelagic clay cores. Sediments around Minamitorishima Island contain > 10 wt% of K-feldspar before ~ 35 Ma, which is five times more than the younger sediments. This distribution does not resemble other volcanic minerals or geochemically estimated volcanic input, suggesting that the K-feldspars are not associated with volcanic ash. The K-feldspars are present as isolated grains as well as pseudorhombohedral microcrystals indicative of authigenic overgrowth. On the other hand, they contain some Na, arguing against a purely authigenic origin. Grain size distributions of chemically separated quartz and feldspars show stratigraphic variation analogous to other North Pacific sites, further suggesting a link to eolian materials. Sediments from a South Pacific site also show K-feldspar enrichment over plagioclase before ~ 44 Ma, although the content relative to bulk sediment does not change much. We propose that the K-feldspar may be enriched in the wide area of the Pacific before ~ 30 to 40 Ma.

Keywords X-ray diffraction, Grain size, Minamitorishima, Site U1366, Ice nucleating particles

1 Introduction

There has been renewed interest in aerosol mineralogy because of the remarkably high ice-nucleating ability of K-feldspar (Atkinson et al. 2013; Harrison et al. 2016). Even though K-feldspar often represents a small fraction (< 5%) of mineral aerosol today, the type, amount, and size of K-feldspar could control the heterogeneous ice nucleation in mixed-phase clouds (e.g. Kanji et al. 2017). This process is critical for cloud microphysics that affects global climate, such as radiative transfer and precipitation. Thus, past changes in ice nucleation activity associated with atmospheric K-feldspar could have affected global paleoclimate, but there is limited evidence for these scenarios. Pankhurst (2017) argued that because granitic upper continental crust contains more K-feldspar than basalt, there should be a Gyr scale secular increase in the dust K-feldspar content following the continental growth. Studying meteorite impact records, Pankhurst et al. (2021) pointed out a positive correlation between the K-feldspar content of the target rock and the associated extinction intensity. They suggested that this correlation reflects global cooling by K-feldspar- rich impact ejecta. However, these hypotheses lack actual relics of eolian K-feldspar. Consequently, the proposed high ice nucleation activity could not be tested.

Pelagic sediments are long-term archives of atmospheric dust including continental materials and volcanic ash (e.g. Rea 1994; Dunlea et al. 2015b). However, little attention has been paid to the detailed feldspar

*Correspondence:
Yoichi Usui
usui-yoichi@se.kanazawa-u.ac.jp
[1] School of Geoscience and Civil Engineering, College of Science and Engineering, Kanazawa University, Nu-7 Kakuma, Kanazawa, Ishiakwa 920-1192, Japan
[2] Volcanoes and Earth's Interior Research Center, Research Institute of Marine Geodynamics, Japan Agency for Marine-Earth Science and Technology (JAMSTEC), 2-15, Natsushima-cho, Yokosuka, Kanagawa 237-0061, Japan
[3] Atmosphere and Ocean Research Institute, The University of Tokyo, 5-1-5 Kashiwanoha, Kashiwa, Chiba 277-8564, Japan

Springer Open

© The Author(s) 2023. **Open Access** This article is licensed under a Creative Commons Attribution 4.0 International License, which permits use, sharing, adaptation, distribution and reproduction in any medium or format, as long as you give appropriate credit to the original author(s) and the source, provide a link to the Creative Commons licence, and indicate if changes were made. The images or other third party material in this article are included in the article's Creative Commons licence, unless indicated otherwise in a credit line to the material. If material is not included in the article's Creative Commons licence and your intended use is not permitted by statutory regulation or exceeds the permitted use, you will need to obtain permission directly from the copyright holder. To view a copy of this licence, visit http://creativecommons.org/licenses/by/4.0/.

mineralogy in marine sediments. Previous studies of dust mineralogy have often focused on clay to decipher continental climate and provenance (Singer 1984). Only a few comprehensive studies have examined bulk sediments or materials treated by HCl (Heath 1969; Peterson and Goldberg 1962). These studies reported low K-feldspar contents that show little temporal variation. In contrast, a recent study of South Pacific pelagic clay using strong chemical digestion to remove clay minerals showed a marked increase in K-feldspar in the deeper (older) section (Usui et al. 2018). However, the chronology of the sediment and the possible origin of the K-feldspars were not thoroughly discussed.

K-feldspar has also been reported from marine sediments as an authigenic phase, often associated with volcanic materials (Bass 1976; Donnelly and Nalli 1973; Kelts and McKinzie 1976; Lancelot et al. 1972; Matthews 1962; Mellis 1952; Stewart et al. 1973). If one wants to use pelagic sediments as archives of past atmospheric dust minerals, it is necessary to distinguish between eolian and authigenic grains. Empirically, authigenic K-feldspars are chemically pure and contain negligible Na and Ca even formed within marine sediments (e.g. Kastner and Siever 1979). They often constitute only a small fraction of the sediments, except some volcaniclastic sediments contain up to 60% K-feldspar (Kelts and McKinzie 1976). Consequently, stratigraphic variations of authigenic K-feldspar in pelagic sediments have not been studied. In pelagic clay, it has been observed that the occurrence of K-feldspar correlates with that of clinoptilolite (Stonecipher 1976). This leads to the suggestion that K-feldspar may form from the diagenesis of clinoptilolite as in saline alkaline lakes (Kastner 1981). However, there is no direct evidence for this reaction in pelagic clays, and it is unclear if they contain authigenic K-feldspar.

Here we present the feldspar mineralogy of two piston cores (KR13-02 PC05 and MR14-02 PC11) collected around Minamitorishima Island, North Pacific. Together with South Pacific data from International Ocean Drilling Program (IODP) Site U1366, our results indicate that K-feldspar is the dominant feldspar for sediments older than Miocene–Oligocene. We discuss the possible origin of the K-feldspars.

2 Materials

We studied two piston cores of pelagic red clay, MR14-E02 PC11 (22° 59.02′ N, 154° 0.98′ E, 5647 m water depth) and KR13-02 PC05 (21° 59.03′ N, 153° 56.35′ E, 5735 m water depth), obtained around Minamitorishima Island (Fig. 1). MR14-E02 PC11 was first dated by Os isotope stratigraphy (Nozaki et al. 2019). Subsequent paleomagnetic studies indicate the low $^{187}Os/^{188}Os$ signature around 34.4 Ma have been spread out after deposition, resulting in a significant overestimation of sedimentation rate (Usui and Yamazaki 2021). Corroborated with Os data and constraints from realistic sedimentation rates, they assign 35–38 Ma at 12.0 m and 30.6–28.1 Ma at 9.0 m. Chronostratigraphy of KR13-02 PC05 was also estimated using Os isotope ratios (Ohta et al. 2020). It has not been examined if the Os isotope signature is affected by post depositional processes as in MR14-E02 PC11. Nonetheless, microfossil ages are broadly consistent with Os isotope data. Therefore, we will use Os isotope ages for sediments younger than 28 Ma, while we rely on magnetostratigraphy or microfossil age constraints before that time. Bulk chemical compositions of cores obtained in this region established regional chemostratigraphy, which divides sediments into five units; unit I to unit V from the youngest to oldest (Tanaka et al. 2020a, b). The chemostratigraphy indicates that KR13-02 PC05 contains sediment much older than MR14-E02 PC11 (Tanaka et al. 2020a). This is also confirmed by our magnetostratigraphy measurements (Fig. 1b, c). The upper part of unit V sediment from different cores contains biogenic magnetite indicative of high surface production (Usui et al. 2018; Yamazaki et al. 2020). Yamazaki et al. (2020) correlate this signature to a paleo-equatorial high-productivity region, ~70 Ma for Minamitorishima. This interpretation indicates that KR13-02 PC05, 9.0 m, may be older than ~70 Ma. Regional acoustic survey (Nakamura et al. 2016) and chemostratigraphic and magnetic correlations (Tanaka et al. 2020a; Yamazaki et al. 2020) indicate that the surface sediment in the studied cores may not be of zero age. The Os isotope data (Nozaki et al. 2019; Ohta et al. 2020) suggests core top ages to be ~2 Ma at 0.014 m in MR14-E02 PC11 and ~11 Ma at 0.11 m in KR13-02 PC05. A hiatus was reported at the boundary between unit I and unit II in MR14-E02 PC11 (Nozaki et al. 2019). In summary, MR14-E02 PC11 covers ~40 to 2 Ma, and KR13-02 PC05 ~70 to 10 Ma.

In addition to the Minamitorishima cores, we reexamined the mineralogy of International Ocean Discovery Program (IODP) Site U1366 in the South Pacific (Expedition 329 Scientists 2011). The sediments in IODP Site U1366 are divided into two lithostratigraphic Units I and II. Unit I is subdivided into three Subunits Ia, Ib, and Ic. Feldspar in Unit Ia is mostly plagioclase. K-feldspar becomes enriched relative to plagioclase down-core (Usui et al. 2018). An age model based on cobalt flux and Os isotope data (Dunlea et al. 2015a, 2021) suggests that the boundary between Unit Ia and Ib may be ~44 Ma, and that for Unit Ib and Unit Ic is ~62 Ma.

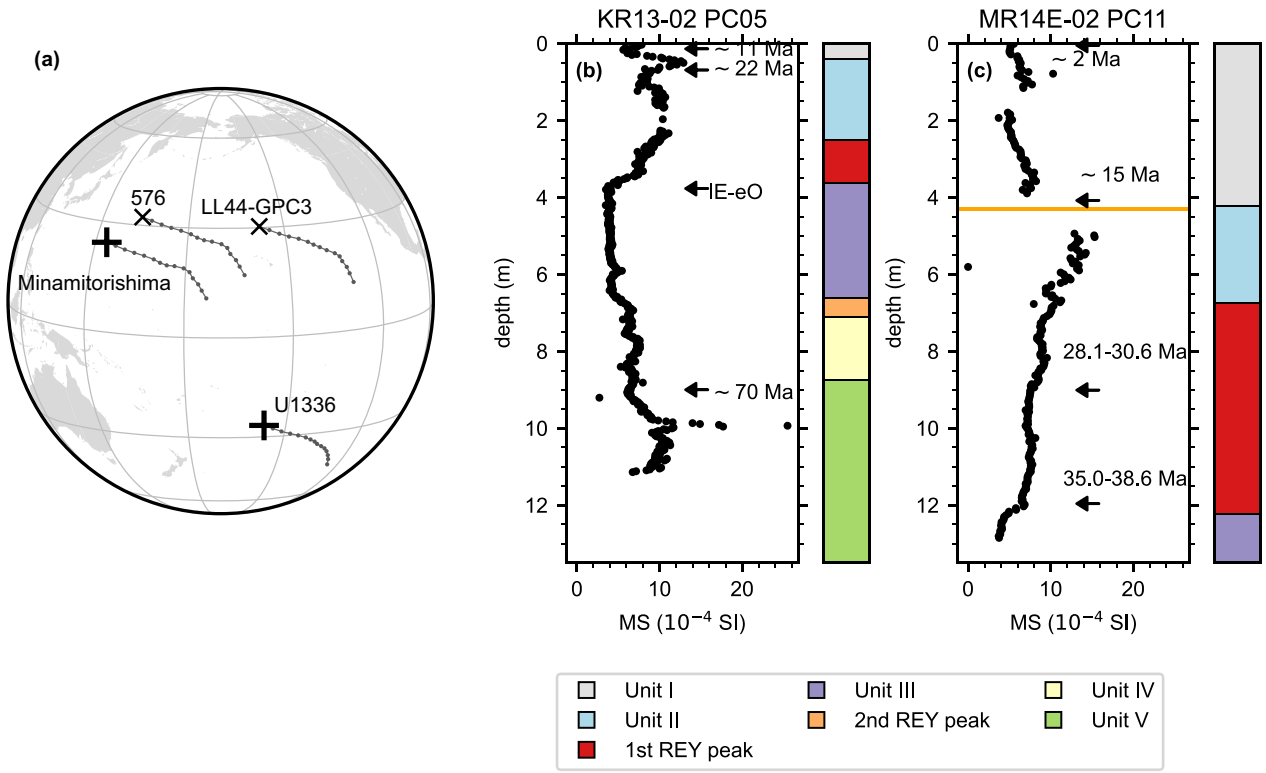

Fig. 1 **a** Map showing the positions and backtracks of the study site (Minamitorishima) and the sites mentioned in the text. Dots represent paleopositions for every 5 Myr back to 70 Ma. Plate motion was calculated using GPlates version 2.3 (https://www.gplates.org) with the rotation model of (Müller et al. 2019). Correlation between **b** KR13-02 PC05 and **c** MR14-E02 PC11 by magnetic susceptibility (MS) and chemostratigraphy (Tanaka et al. 2020a). Magnetic susceptibility was measured with 7 cc cube specimens using Kappabridge (AGICO, KLY-4). Arrows indicate age constraints obtained by ichthyolith stratigraphy (Ohta et al. 2020), Osmium isotopes stratigraphy (Nozaki et al. 2019; Ohta et al. 2020), and magnetostratigraphy (Usui and Yamazaki 2021). lE stands for late Eocene, and eO for early Oligocene. Orange horizontal line in **c** indicates a hiatus

3 Methods

3.1 Chemical digestion

We performed digestion by citrate-bicarbonate-dithionite (CBD) (Rea and Janecek 1981) and sodium pyrosulfate fusion to extract feldspar and quartz (Inoue et al. 2021; Kiely and Jackson 1964; Syers et al. 1968; Usui et al. 2018). Dry samples of ~1 g were first treated with CBD to remove poorly crystalline Fe–Mn oxyhydroxides. The residues were washed with purified water, freeze-dried, and weighed. The oxyhydroxide-free residues were then subjected to the sodium pyrosulfate fusion as follows. First, the residues were fused with $Na_2S_2O_7$ at 460 °C to decompose sheet silicates. Next, the fusions were treated with 3N HCl and washed with purified water. Then, the residues were heated to 50 °C in 1 M NaOH overnight to remove relict clays. The sodium pyrosulfate fusion was repeated 2 or 3 times to ensure complete digestion. While the CBD and acetic acid treatments have been widely used to extract the eolian component from pelagic sediments, these methods were ineffective in removing biogenic apatite (Usui and Yamazaki 2021) and authigenic zeolite (Ziegler et al. 2007), even though those phases sometimes account for over 30 vol% of the sediment in the studied region (Iijima et al. 2016; Ohta et al. 2020). Strong acid treatment should dissolve biogenic apatite while preserving quartz, but it is not yet clear if the pyrosulfate fusion would remove all clay minerals and zeolite and if it would attack feldspars. While we focus on the pyrosulfate fusion residues, we also compare materials obtained by the CBD treatment and bulk, untreated materials to examine the effect of pyrosulfate fusion. In any case, the materials analyzed in this study should be regarded as operationally defined components.

3.2 Mineralogy

We examined the mineralogy of the pyrosulfate fusion residues by X-ray diffraction (XRD). XRD measurements used a diffractometer (MiniFlex II, Rigaku) with Cu Kα radiation. To check the potential effect of chemical digestion on the mineralogy, we also measured selected samples in untreated conditions and after the CBD treatment. We estimate mineral proportions by the Reference

Intensity Ratio method with full pattern summation using the software PowdR (Butler and Hillier 2021). We used reference patterns of K-feldspar, plagioclase, quartz, and clinoptilolite from the RockJock reference library (Eberl 2003). We also included glass, tephra, and obsidian reference patterns because some samples revealed a broad peak. We will call them collectively "glass"; however, it is introduced to fit the observed background of the spectra, and not much interpretation should be made on this phase. We also reexamine the XRD data from IODP Site U1366C (Usui et al. 2018) using the same protocol. The fusion residues were also examined under a scanning electron microscope (SEM; JEOL JSM-6010V) equipped with an energy-dispersive spectrometer EDS.

3.3 Grain size

Grain size distributions were measured for the fusion residues. The samples were first dispersed in a 0.2% sodium hexametaphosphate and sonicated for 1 h. Then the dispersed sample was introduced into a laser diffraction particle size analyzer (Mastersizer 3000E, Malvern Panalytical) with purified water.

4 Results

The CBD treatment reduces the sample weight by 10–20%. Sodium pyrosulfate fusion further reduces the sample weight to 10–30% of the original weight.

The XRD spectrograms can be fitted with the selected phases in various proportions (Figs. 2 and 5). The only

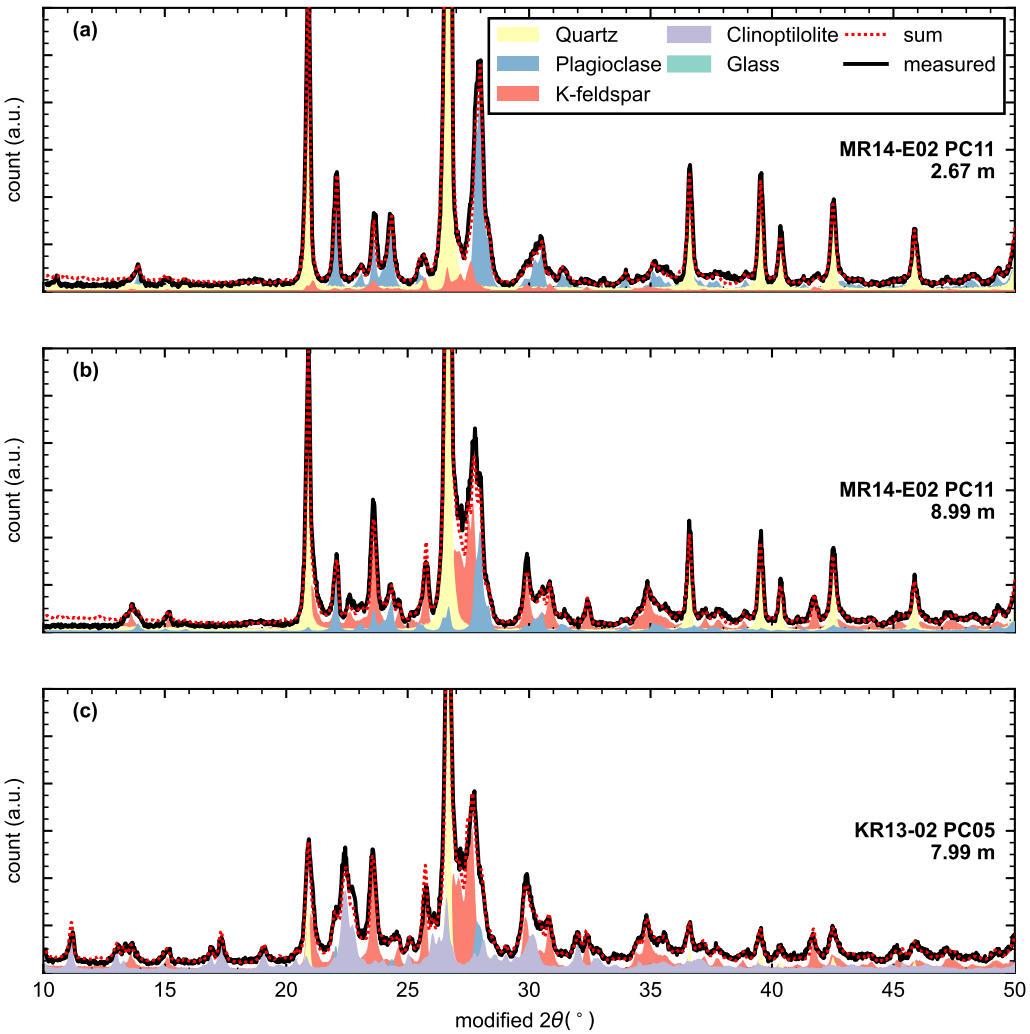

Fig. 2 XRD diffractograms of fusion residues and their fits of **a** MR14-E02 PC11, 2.67 m, **b** MR14-E02 PC11, 8.99 m, and **c** KR13-02 PC05, 8.01 m. Data are on the modified 2θ angles calculated by the PowdR software. The quartz peak at 26.6° is out of bounds

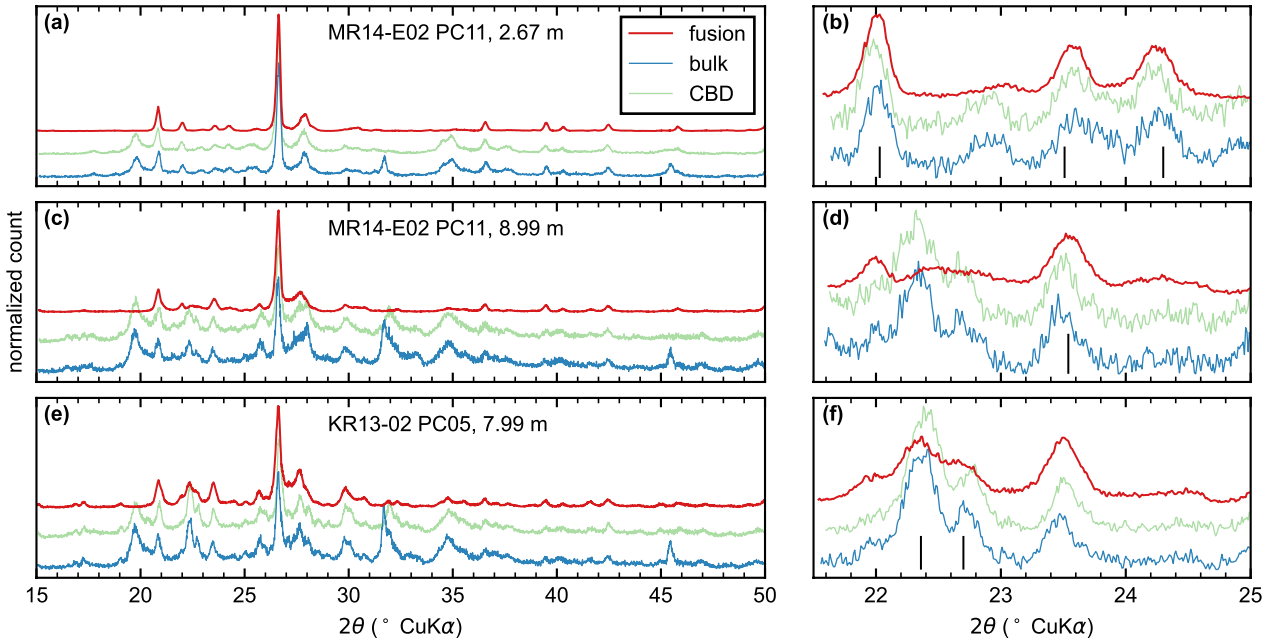

Fig. 3 The effect of chemical treatments on the XRD diffractogram of **a**, **b** MR14-E02 PC11, 2.67 m, **c**, **d** MR14-E02 PC11, 8.99 m, and **e**, **f** KR13-02 PC05 7.99 m. Blue, green, and red lines show untreated samples, samples after CBD treatment, and samples after sodium pyrosulfate fusion treatment. The spectra was aligned and normalized using the quartz peak at about 26.6°. Black vertical lines are diagnostic peak positions for plagioclase (**b**), K-feldspar (**d**), and clinoptilolite (**f**)

exceptions are KR13-02 PC05, 2.66 m, KR13-02 PC05, 2.79 m, and U1366C-2H-5W, 143 cm, which indicate the presence of small amount of additional phases (Additional file 1). These samples are excluded from further discussion. We cannot completely exclude the presence of additional phases in the other samples, but the XRD spectra suggest that those unspecified phases should be minor components. Large variations in K-feldspar content relative to plagioclase are also evident from spectra for bulk sediments before chemical digestion (Fig. 3). This result confirms that the digestion treatments are not the primary reason for the variations in K-feldspar content. SEM/EDS analyses confirmed the presence of K-feldspar (K-rich Al silicate) as well as plagioclase (Na-rich Al silicate) and quartz (Fig. 4). K-feldspar appears as isolated grains (Fig. 4b) and grains covered by rhombohedral crystals similar to authigenic K-feldspar (e.g. Worden and Rushton 1992) (Fig. 4c). The resolution of the SEM limits detailed observations to grains over a few microns, which is larger than the median grain size. Both types of K-feldspar appear to contain Na. However, each rhombohedral crystal is too small to be measured separately, and the signature may reflect submicroscopic heterogeneity. The quartz grains are more surrounded compared to the feldspars (Fig. 4e). Otherwise, there is no significant difference in size or morphology between the minerals. The mass fraction of fusion residue and mineral proportions within the residue show systematic stratigraphic variations. In the Minamitorishima cores, the fraction of the residues is the smallest around 30–35 Ma (Fig. 5a, c). In terms of feldspar mineralogy, all cores are dominated by plagioclase in the shallow part, while K-feldspar is enriched over plagioclase in the deep part. K-feldspar enrichment occurs before ~28 to 39 Ma (including late Eocene to early Oligocene in KR13-02 PC05) for Minamitorishima cores, while it occurs before ~44 Ma for IODP site U1366 (Fig. 5b, d, f).

Some intervals show signs of increased volcanic input, but this does not cover the entire interval where K-feldspar is enriched. A few samples contain a high proportion of glass within the fusion residue (Fig. 5b, d). These intervals, i.e. ~6 m in MR14-E02 PC11 and ~3 m in KR13-02 PC05, correspond to the so-called "extremely REY-rich mud" interval (Iijima et al. 2016), where the biogenic apatite content reaches ~30 wt%. Samples below 8.1 m in KR13-02 PC05 contain significant clinoptilolite (Fig. 5d), a diagenetic mineral likely derived from volcanic glass (Lisitzina and Butuzova 1982; Petzing and Chester 1979). In addition, it should be noted that some volcanic glass and zeolite are likely to be removed during

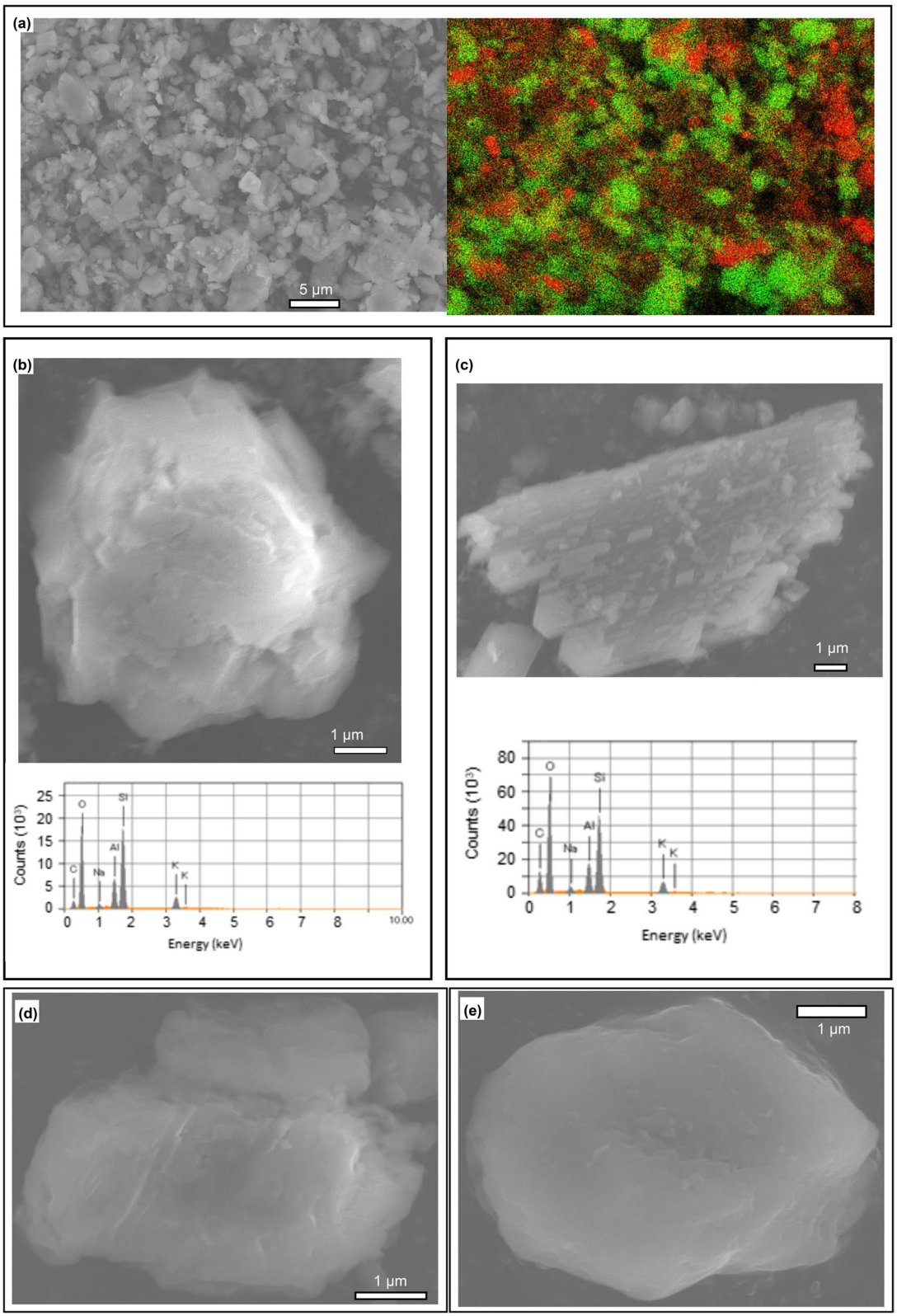

Fig. 4 SEM images of KR13-02 PC05, 5.04 m. **a** Image (left) and element map (right) of grains. Green shows K, and red shows Na. **b** An isolated grain of K-feldspar together with the EDS spectra. **c** A grain covered by rhombohedral crystals. **d** Plagioclase. **e** Quartz

chemical treatment. In particular, phillipsite has been reported to constitute up to 30% of bulk samples at 1.6–2.0 m in KR13-02 PC05 (Ohta et al. 2016, 2020), but it is not detected in our digested samples. However, these variations are not in phase with the consistently high K-feldspar fraction below 4 m in KR13-02 PC05 (Fig. 5b), suggesting that the K-feldspars are not direct volcanic input.

We calculate the mineral content relative to the bulk sediments using the mass fraction of fusion residues and the mineral proportions within the residues. In the Minamitorishima cores, the calculated K-feldspar content reaches 12 wt% of the bulk sediments in the deeper stratigraphic level, while it is about 2 wt% in the shallower level (Fig. 6). At IODP Site U1366, the K-feldspar content does not vary much because the low proportion of fusion residues in Unit Ib (Fig. 5e) (Usui et al. 2018) compensates for the high proportion of K-feldspar in the fusion residues.

Grain size distributions of the fusion residues generally show the mode at 2 μm to 4 μm (Fig. 7). Smaller grain size with the mode at ~2 μm is observed in MR14-E02 PC11 below 11.99 m and in KR13-02 PC05 between 3.87 m to 7.05 m. These grain size variations resemble that of the eolian dust in the North Pacific (Janecek 1985; Janecek and Rea 1983), where the grain size is finer between ~50 and ~30 Ma (Fig. 7e). The depth of the grain size change (11.99 m in MR14-E02 PC11) is different from that of the mineralogical change (7 m). Thus, we interpret these changes reflect original grain size variations, even though it may be possible that the grain sizes are reduced by the chemical digestion. Some samples show bimodal grain size distribution with another maxima at ~20 μm, possibly reflecting sorting by strong bottom current (McCave et al. 1995; Ohta et al. 2016).

5 Discussion

We discovered large variations in K-feldspar content from North Pacific red clay. Together with the South Pacific data (Usui et al. 2018), it appears that Pacific red clay before ~30 to 40 Ma is enriched in K-feldspar relative to plagioclase. Moreover, in the North Pacific sites, K-feldspar is a major component (>10 wt%) of the bulk sediments at that time. The most probable origin of the K-feldspars seems to be either eolian or a replacement of eolian plagioclase. Although K-feldspar may form after volcanic materials (Kelts and McKinzie 1976; Lancelot et al. 1972; Mellis 1952), they are not enough to explain the K-feldspar enrichment. Clinoptilolite content is only significant in the lowermost part of KR13-02 PC05 and does not correlate with K-feldspar content (Fig. 5d). A modeling study using bulk chemistry also suggests the mass fraction of a volcanic component is limited to be<10 wt% between 4 and 7 m and ~20 wt% below 8 m (Tanaka et al. 2022). In contrast, K-feldspar content already reaches ~10 wt% between 4 and 7 m in the core (Fig. 6b). These contrasting variations are difficult to explain with K-feldspar formed after volcanic materials.

Eolian transport of the K-feldspars is a natural explanation for their variable abundance. Changes in either provenance or weathering conditions in the source area can result in mineralogical changes. Indeed, mid- and low-latitude sites in the North Pacific often show provenance changes around 25–45 Ma due to a change in zonal wind patterns or plate migration (Hyeong et al. 2016; Kyte et al. 1993; Pettke et al. 2002; Ziegler and Murray 2007). This timing coincides with the transition from K-feldspar-rich to plagioclase-rich sediments at the Minamitorishima sites. The similarity between grain size variations of chemical digestion residues and previously reported atmospheric dust records in the North Pacific (Janecek 1985; Janecek and Rea 1983) (Fig. 7e) further suggests that the K-feldspars are related to eolian dust. However, further mineral-specific measurements are needed to conclude this point. The variations in the eolian flux in the North Pacific are less than a factor of 2 between 45 and 10 Ma (Janecek 1985; Janecek and Rea 1983). This is much smaller than the observed variations in K-feldspar content, which reach a factor of 5. Thus, if the majority of the K-feldspar is of eolian origin, the atmospheric dust before ~28 to 39 Ma would have contained much more K-feldspar than younger times. Because K-feldspar has high ice nucleation potential and dominating the ice formation by silicate dust, our results suggest that clouds over the Pacific before ~28 to 39 Ma tends to glaciate more easily.

Alternatively to simple eolian transport of K-feldspar, formation after eolian plagioclase may explain the observations. Although this reaction has not been considered for pelagic clay, the microtexture (Fig. 4c) indicates that at least some of the K-feldspars are formed through the authigenic overgrowth. Formation via dissolution and precipitation could convert plagioclase into isolated K-feldspar grains (e.g. Putnis and John 2010) and explain the grain size variations, even though we do not have positive evidence for authigenic origin for such isolated grains (Fig. 4b). Chemical composition data from isolated K-feldspars (Fig. 4b) argue against a diagenetic origin, as diagenetic K-feldspar has been reported to be chemically pure with minimal Na or Ca substitutions. However, we cannot rule out possible averaging over submicroscopic heterogeneity in authigenic replacement. Detailed microscopic work would clarify their origin (e.g. Lee and Parsons 2003). It should be noted that the studied sites

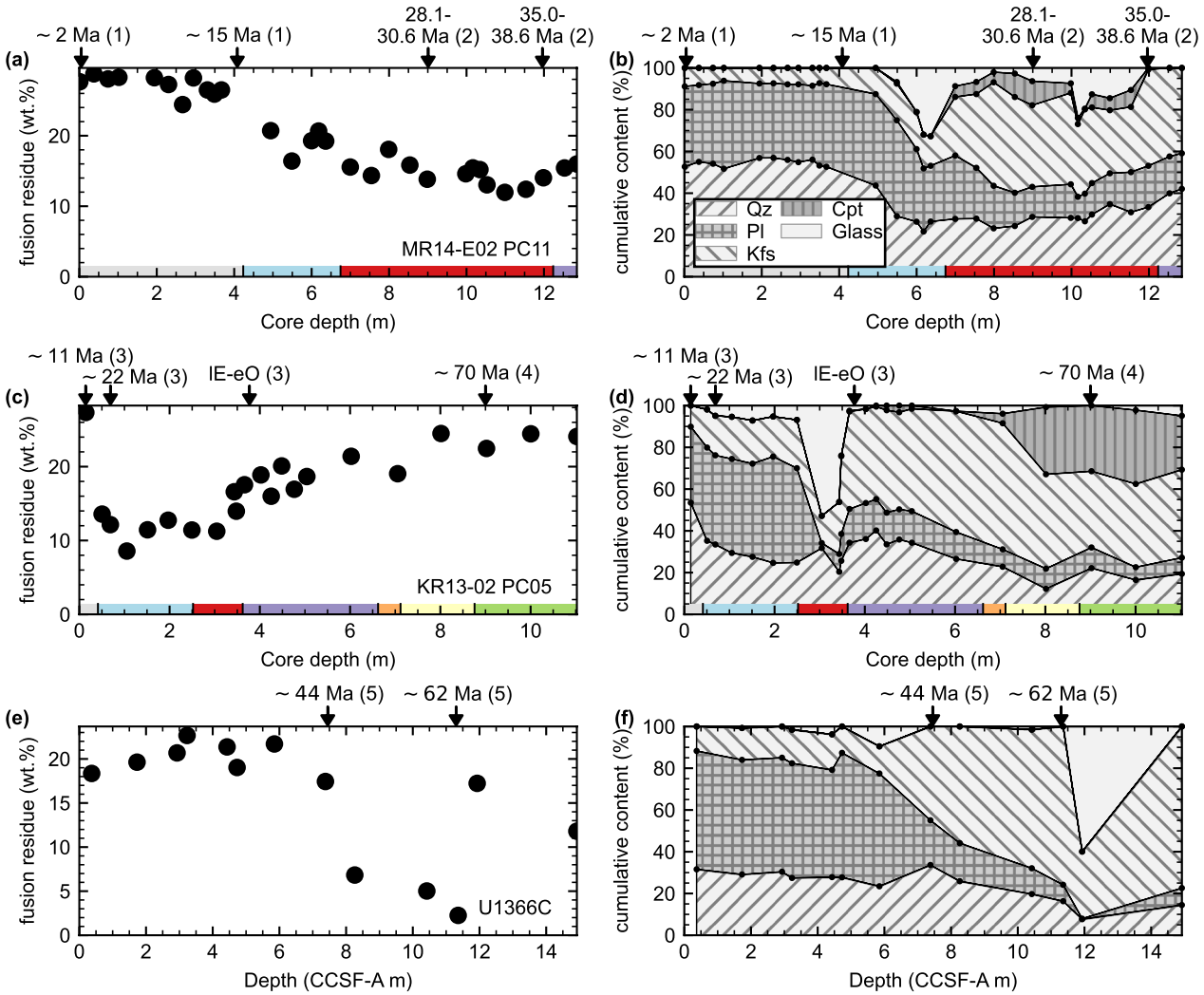

Fig. 5 Stratigraphic variation of the fusion residues. **a**, **c**, **e** Mass fraction of the fusion residues for **a** MR14-E02 PC11, **c** KR13-02 PC05, and **e** IODP Site U1366 (Usui et al. 2018). **b**, **d**, **f** Stack plots showing mineral proportions in the fusion residues of **b** MR14-E02 PC11, **e** KR13-02 PC05, and **e** IODP Site U1366 (Usui et al. 2018). Ages are based on (1) Nozaki et al. (2019), (2) Usui and Yamazaki (2021), (3) Ohta et al. (2020), (4) Yamazaki et al. (2020), and (5) Dunlea et al. (2015a). Qz: Quartz, Pl: Plagioclase, Kfs: K-feldspar, Cpt: Clinoptilolite. The chemostratigraphic units (Tanaka et al. 2020a) are shown at the top of **a**, **b**, **c**, and **d**. For a color cord, see Fig. 1

are distributed within narrow paleolatitudes (Fig. 1a), where provenance changes around 25–45 Ma have been reported (Hyeong et al. 2016; Kyte et al. 1993; Pettke et al. 2002; Ziegler and Murray 2007). Examination of samples outside this latitudinal band would test if the K-feldspar enrichment reflect time-dependent authigenic reactions or eolian mineralogy reflecting dust provenance.

6 Conclusions

Pelagic clays around Minamitorishima Island, western North Pacific, contain varying amounts of K-feldspar. Before ~35 Ma it is > 10%, while after ~15 Ma it is 2–3% (Fig. 6). IODP Site U1366C in the South Pacific also shows K-feldspar enrichment over plagioclase before ~44 Ma (Usui et al. 2018), but its concentration in the bulk sediments is not particularly high. Volcanic glass and zeolite show stratigraphic variations different from K-feldspar. Previous geochemical data suggest that volcanic input is less than the mass fraction of K-feldspar. Thus, we conclude that K-feldspar is not directly associated with volcanic input such as tephra. The K-feldspar appears to contain Na, in contrast to nearly pure authigenic feldspars (Kastner and Siever 1979), although we cannot rule out nanoscale heterogeneity. Grain size variations of chemically separated feldspars and quartz are similar to those of eolian dust in the North Pacific (Fig. 7)

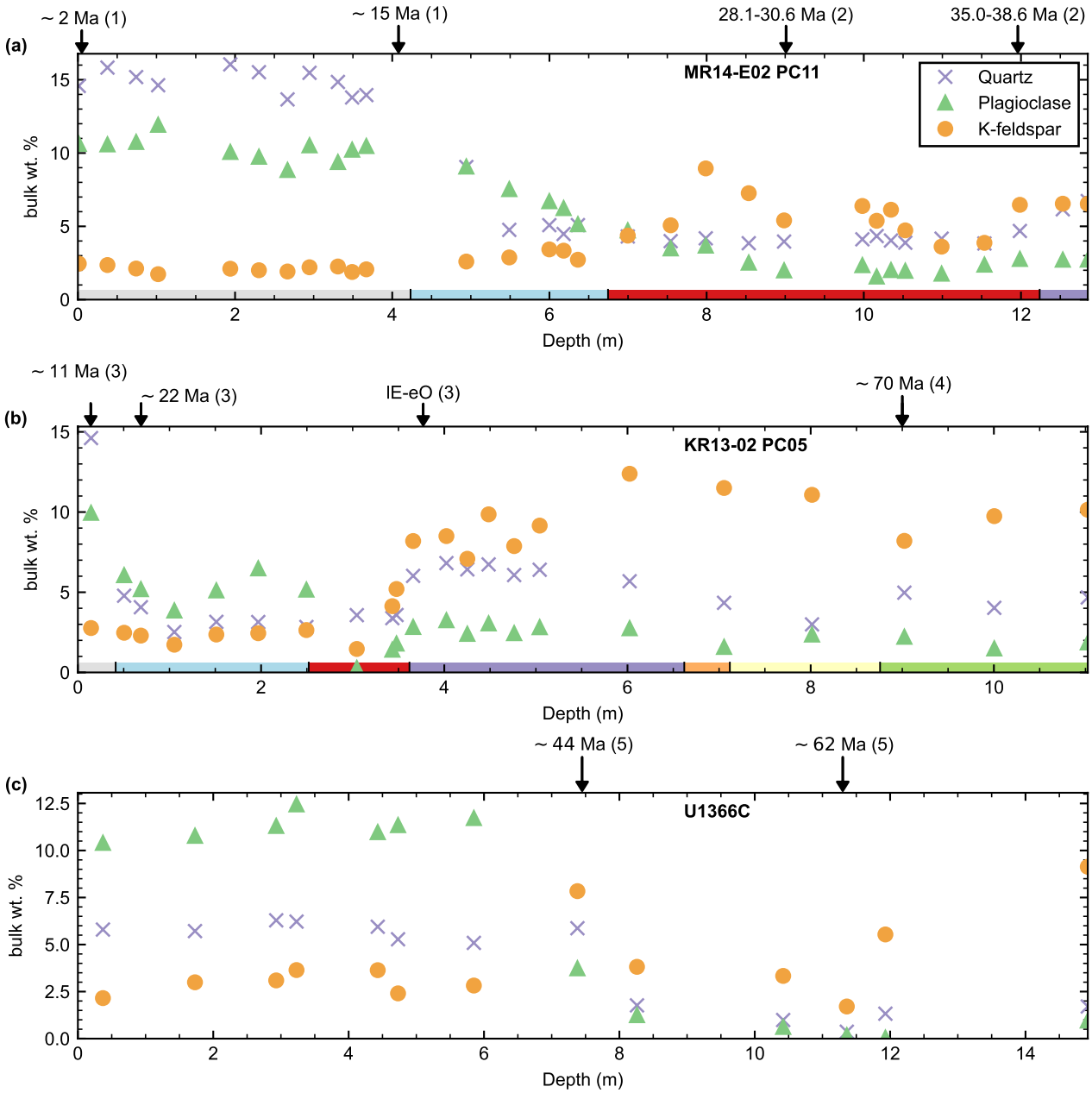

Fig. 6 Estimated mineral content in the bulk samples based on the XRD results and weight of fusion residues for **a** MR14-E02 PC11, **b** KR13-02 PC05, and **c** IODP Site U1366C. Ages are based on (1) Nozaki et al. (2019), (2) Usui and Yamazaki (2021), (3) Ohta et al. (2020), (4) Yamazaki et al. (2020), and (5) Dunlea et al. (2015a). The chemostratigraphic units (Tanaka et al. 2020a) are shown at the top of **a** and **b**. For a color cord, see Fig. 1

(Janecek 1985; Janecek and Rea 1983). These observations can be explained either by the eolian origin of the K-feldspars or by authigenic formation replacing eolian plagioclase. If they are eolian dust, then our data indicate that the past atmospheric dust had much higher ice-nucleating activity than modern dust. Alternatively, if the K-feldspar is of authigenic origin, the use of pelagic clays as archives of past eolian dust minerals should be reconsidered. Further study in geographic distribution of K-feldspar enrichment is warranted to constrain past atmospheric dust and potentially widespread redistribution of Na and K within pelagic sediments.

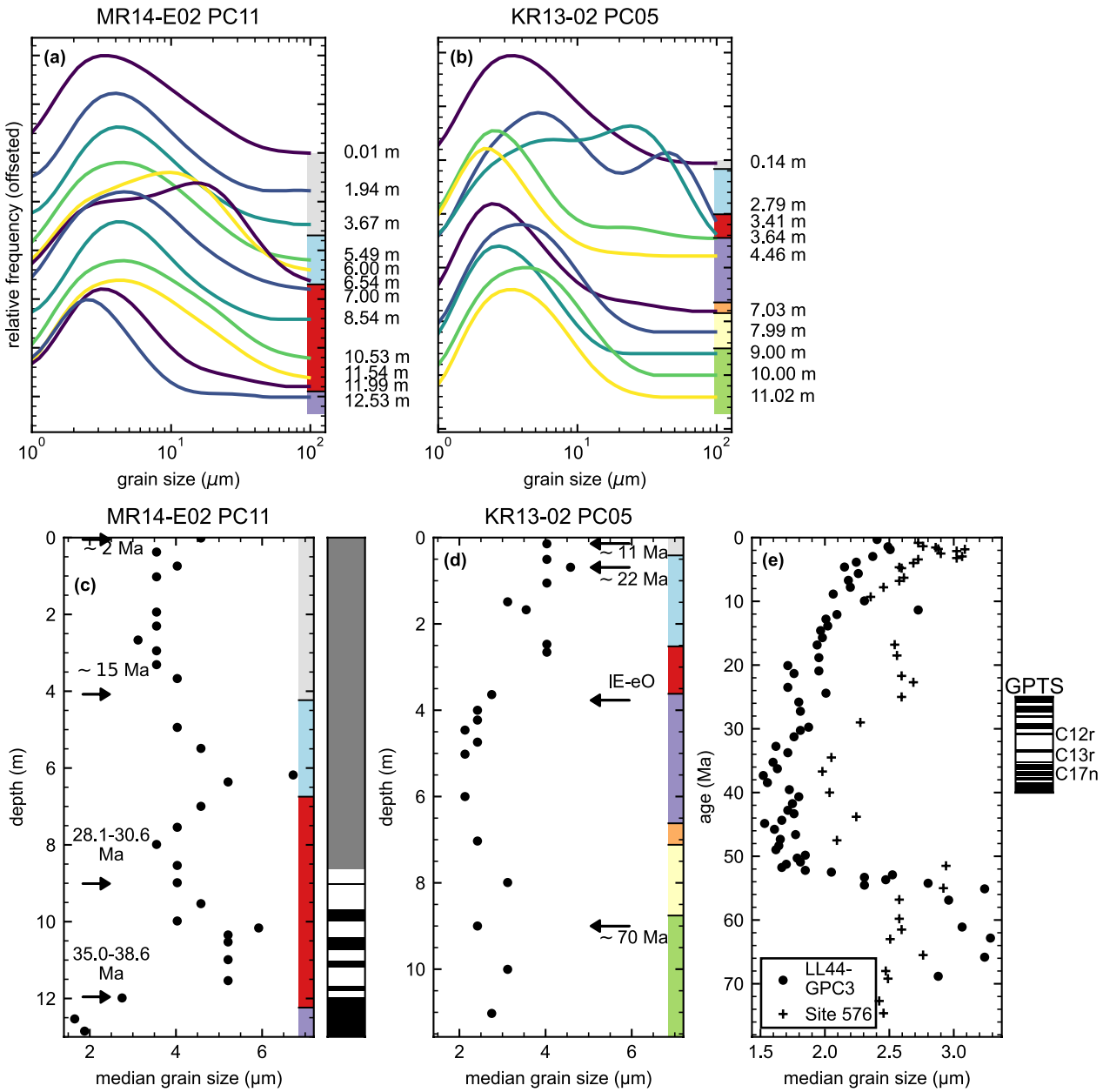

Fig. 7 **a**, **b** Grain size distributions of selected fusion residues of **a** MR14-E01 PC11 and **b** KR13-02 PC05. Data are offset according to their depth, and the depth of each sample is indicated on the right. **c**, **d** Depth variation of median grain size from **c** MR14-E02 PC11 and **d** KR13-02 PC05. Samples with bimodal grain size distributions were not plotted. The paleomagnetic polarity zones of Usui and Yamazaki (2021) are shown on the right of **c**. Black indicates normal polarity, white indicates reversed polarity, and gray indicates a zone with an uncertain polarity pattern. **e** Temporal variation of median grain size from LL44-GPC3 (Janecek and Rea 1983) and DSDP Site 576 (Janecek 1985). The geomagnetic polarity timescale (GPTS) between 40 and 25 Ma (Ogg 2020) is shown on the right. The chemostratigraphic units (Tanaka et al. 2020a) are shown on the right of **c** and **d**. For a color cord, see Fig. 1

Abbreviations

IODP	Integrated Ocean Drilling Program
ODP	Ocean Drilling Program
DSDP	Deep-Sea Derilling Program
CBD	Citrate-bicarbonate-dithionite
EOT	Eocene–Oligocene Transition
ITCZ	Intertoropical convergence zone
XRD	X-ray diffraction
REY	Rare-earth elements and yttrium

Supplementary Information

The online version contains supplementary material available at https://doi.org/10.1186/s40645-023-00581-z.

Additional file 1. Samples with poorly fitted XRD diggractogram. **A**. KR13-02 PC05, 2.66 m, showing unfitted peaks at around 19° and 38°. B. KR13-02 PC05, 2.79 m, showing ill-fitted peaks at around 13° and 27°. **B**. U1366C-2H-5W, 143 cm, showing multiple peaks fitted with insufficient intensity between 20°–35°. **C**. U1366C-2H-5W, 143 cm, showing peaks at around 21°, 24°, and 29° fitted with insufficient intensity.

Acknowledgements
We thank Yasuhiro Takashimizu and Jyonaotaro Onodera for their instructions and help in grain size measurements.

Author contributions
YU made contributions to conceptualization, methodology, formal analysis, investigation, and wiring—original draft. TY made contributions to conceptualization, writing—review and editing.

Funding
This study was supported by JSPS KAKENHI Grant Nos. JP17H01361 and JP19H01997.

Availability of data and materials
The datasets supporting the conclusions of this article are available in the Zenodos repository at https://doi.org/10.5281/zenodo.8210625.

Declarations

Competing interests
The authors declare that they have no competing interests.

Received: 7 April 2023 Accepted: 3 August 2023
Published online: 14 August 2023

References

Atkinson JD, Murray BJ, Woodhouse MT, Whale TF, Baustian KJ, Carslaw KS, Dobbie S, O'Sullivan D, Malkin TL (2013) The importance of feldspar for ice nucleation by mineral dust in mixed-phase clouds. Nature 498:355–358. https://doi.org/10.1038/nature12278

Bass, M.N (1976) Secondary Minerals in Oceanic Basalts, with Special Reference to Leg 34, Deep Sea Drilling Project. In: Initial Reports of the Deep Sea Drilling Project. U.S. Government Printing Office, Washington D.C. https://doi.org/10.2973/dsdp.proc.34.128.1976.

Butler BM, Hillier S (2021) powdR: an R package for quantitative mineralogy using full pattern summation of X-ray powder diffraction data. Comput Geosci 147:104662. https://doi.org/10.1016/j.cageo.2020.104662

Donnelly, T.W, Nalli, G (1973) Mineralogy and Chemistry of Caribbean Sediments. In: Initial Reports of the Deep Sea Drilling Project, 15. U.S. Government Printing Office, Washington, D.C. https://doi.org/10.2973/dsdp.proc.15.127.1973.

Dunlea AG, Murray RW, Sauvage J, Pockalny RA, Spivack AJ, Harris RN, D'Hondt S (2015a) Cobalt-based age models of pelagic clay in the south pacific gyre. Geochem Geophys Geosyst 16(8):2694–2710. https://doi.org/10.1002/2015gc005892

Dunlea AG, Murray RW, Sauvage J, Spivack AJ, Harris RN, D'Hondt S (2015b) Dust, volcanic ash, and the evolution of the South Pacific Gyre through the Cenozoic. Paleoceanography 30(8):1078–1099. https://doi.org/10.1002/2015PA002829

Dunlea AG, Tegler LA, Peucker-Ehrenbrink B, Anbar AD, Romaniello SJ, Horner TJ (2021) Pelagic clays as archives of marine iron isotope chemistry. Chem Geol 575:120201. https://doi.org/10.1016/j.chemgeo.2021.120201

Eberl DD (2003) User Guide to RockJock - A Program for Determining Quantitative Mineralogy from X-Ray Diffraction Data. US Geological Survey. https://doi.org/10.3133/ofr200378

Expedition 329 Scientists (2011) Site u1366. In: Proceedings of the IODP. Integrated Ocean Drilling Program, College Station. https://doi.org/10.2204/iodp.proc.329.104.2011.

Harrison AD, Whale TF, Carpenter MA, Holden MA, Neve L, O'Sullivan D, Temprado JV, Murray BJ (2016) Not all feldspars are equal: a survey of ice nucleating properties across the feldspar group of minerals. Atmos Chem Phys 16(17):10927–10940. https://doi.org/10.5194/acp-16-10927-2016

Heath GR (1969) Mineralogy of Cenozoic Deep-Sea Sediments from the Equatorial Pacific Ocean. Geol Soc Am Bull 80(10):1997–2018. https://doi.org/10.1130/0016-7606(1969)80[1997:mocdsf]2.0.co;2

Hyeong K, Kuroda J, Seo I, Wilson PA (2016) Response of the Pacific inter-tropical convergence zone to global cooling and initiation of Antarctic glaciation across the Eocene Oligocene Transition. Sci Rep 6:30647. https://doi.org/10.1038/srep30647

Iijima K, Yasukawa K, Fujinaga K, Nakamura K, Machida S, Takaya Y, Ohta J, Haraguchi S, Nishio Y, Usui Y et al (2016) Discovery of extremely REY-rich mud in the western North Pacific Ocean. Geochem J 50(6):557–573. https://doi.org/10.2343/geochemj.2.0431

Inoue K, Yamazaki T, Usui Y (2021) Influence of magnetofossils on paleointensity estimations inferred from principal component analyses of first-order reversal curve diagrams for sediments from the western equatorial Pacific. Geochem Geophys Geosyst 22(10):e2021GC010081. https://doi.org/10.1029/2021gc010081

Janecek TR, Rea DK (1983) Eolian deposition in the northeast Pacific Ocean: Cenozoic history of atmospheric circulation. Geol Soc Am Bull 94(6):730–738. https://doi.org/10.1130/0016-7606(1983)94%3c730:EDITNP%3e2.0.CO;2

Janecek TR (1985) Eolian sedimentation in the Northwest Pacific ocean: a preliminary examination of the data from deep sea drilling project sites 576 and 578. In: Heath GR, Burckle LH, D'Agostino AE et al (eds) Initial Reports DSDP Volume 86. U.S. Government Printing Office, Washington, D.C., pp 859–603. https://doi.org/10.2973/dsdp.proc.86.126.1985.

Kanji ZA, Ladino LA, Wex H, Boose Y, Burkert-Kohn M, Cziczo DJ, Kr¨amer, M, (2017) Overview of Ice Nucleating Particles. Meteorol Monogr 58:1–33. https://doi.org/10.1175/amsmonographs-d-16-0006.1

Kastner M (1981) The sea. In: Emiliani C (ed) Authigenic silicates in deep-sea sediments: formation and diagenesis. The Oceanic Lithosphere, vol 7. Wiley, New York, pp 915–980

Kastner M, Siever R (1979) Low temperature feldspars in sedimentary rocks. Am J Sci 279(4):435–479. https://doi.org/10.2475/ajs.279.4.435

Kelts K, McKinzie JA (1976) Cretaceous volcanogenic sediments from the line Islands Chain: diagenesis and formation of K-Feldspar, DSDP Leg 33, Hole 315A and Site 316. In: Initial Reports of the Deep Sea Drilling Project, 33. U.S. Government Printing Office, Washington, D.C. https://doi.org/10.2973/dsdp.proc.33.128.1976

Kiely PV, Jackson ML (1964) Selective dissolution of micas from potassium feldspars by sodium pyrosulfate fusion of soils and sediments. Am Miner 49(11–12):1648–1659

Kyte FT, Leinen M, Heath GR, Zhou L (1993) Cenozoic sedimentation history of the central North Pacific: inferences from the elemental geochemistry of core LL44-GPC3. Geochim Cosmochim Acta 57(8):1719–1740. https://doi.org/10.1016/0016-7037(93)90109-A

Lancelot Y, Hathaway JC, Hollister CD (1972) Lithology of sediments from the western North Atlantic, Leg XI, Deep Sea Drilling Project. In: Initial reports of the deep sea drilling project, 11. U.S. Government Printing Office, Washington, D.C. https://doi.org/10.2973/dsdp.proc.11.131.1972

Lee MR, Parsons I (2003) Microtextures of authigenic Or-rich feldspar in the Upper Jurassic Humber Group, UK North. Sea Sedimentol 50(3):597–608. https://doi.org/10.1046/j.1365-3091.2003.00567.x

Lisitzina NA, Butuzova GY (1982) Authigenic zeolites in the sedimentary mantle of the world ocean. Sed Geol 31(1):33–41. https://doi.org/10.1016/0037-0738(82)90005-7
Matthews DH (1962) Altered lavas from the floor of the eastern North Atlantic. Nature 194(4826):368–369. https://doi.org/10.1038/194368a0
McCave IN, Manighetti B, Robinson SG (1995) Sortable silt and fine sediment size/composition slicing: parameters for palaeocurrent speed and palaeoceanography. Paleoceanography 10(3):593–610. https://doi.org/10.1029/94pa03039
Mellis O (1952) Replacement of plagioclase by orthoclase in deep-sea deposits. Nature 169:624–624. https://doi.org/10.1038/169624a0
Müller RD, Zahirovic S, Williams SE, Cannon J, Seton M, Bower DJ, Tetley MG, Heine C, Breton EL, Liu S, Russell SHJ, Yang T, Leonard J, Gurnis M (2019) A global plate model including lithospheric deformation along major rifts and orogens since the triassic. Tectonics 38(6):1884–1907. https://doi.org/10.1029/2018tc005462
Nakamura K, Machida S, Okino K, Masaki Y, Iijima K, Suzuki K, Kato Y (2016) Acoustic characterization of pelagic sediments using sub-bottom profiler data: Implications for the distribution of REY-rich mud in the Minamitorishima EEZ, western Pacific. Geochem J 50(6):605–619. https://doi.org/10.2343/geochemj.2.0433
Nozaki T, Ohta J, Noguchi T, Sato H, Ishikawa A, Takaya Y, Kimura J-I, Chang Q, Shimada K, Ishibashi J-i et al (2019) A Miocene impact ejecta layer in the pelagic Pacific Ocean. Sci Rep 9:16111. https://doi.org/10.1038/s41598-019-52709-1
Ogg JG (2020) Geomagnetic Polarity Time Scale. In: Gradstein FM, Ogg JG, Schmitz MD, Ogg GM (eds) Geologic Time Scale 2020, vol 1. Elsevier, Amsterdam, pp 159–192. https://doi.org/10.1016/b978-0-12-824360-2.00005-x
Ohta J, Yasukawa K, Machida S, Fujinaga K, Nakamura K, Takaya Y, Iijima K, Suzuki K, Kato Y (2016) Geological factors responsible for REY-rich mud in the western North Pacific Ocean: Implications from mineralogy and grain size distributions. Geochem J 50(6):591–603. https://doi.org/10.2343/geochemj.2.0435
Ohta J, Yasukawa K, Nozaki T, Takaya Y, Mimura K, Fujinaga K, Nakamura K, Usui Y, Kimura J-I, Chang Q et al (2020) Fish proliferation and rare-earth deposition by topographically induced upwelling at the late Eocene cooling event. Sci Rep 10:9896. https://doi.org/10.1038/s41598-020-66835-8
Pankhurst MJ (2017) Atmospheric K-feldspar as a potential climate modulating agent through geologic time. Geology 45(4):379–382. https://doi.org/10.1130/g38684.1
Pankhurst MJ, Stevenson CJ, Coldwell BC (2021) Meteorites that produce K-feldspar-rich ejecta blankets correspond to mass extinctions. J Geol Soc 179(3):jgs2021-055. https://doi.org/10.1144/jgs2021-055
Peterson MNA, Goldberg ED (1962) Feldspar distributions in South Pacific pelagic sediments. J Geophys Res 67(9):3477–3492. https://doi.org/10.1029/jz067i009p03477
Pettke T, Halliday AN, Rea DK (2002) Cenozoic evolution of Asian climate and sources of Pacific seawater Pb and Nd derived from eolian dust of sediment core LL44-GPC3. Paleoceanography 17(3):3–1. https://doi.org/10.1029/2001PA000673
Petzing J, Chester B (1979) Authigenic marine zeolites and their relationship to global volcanism. Mar Geol 29(1–4):253–271. https://doi.org/10.1016/0025-3227(79)90112-9
Putnis A, John T (2010) Replacement processes in the Earth's crust. Elements 6(3):159–164. https://doi.org/10.2113/gselements.6.3.159
Rea DK (1994) The paleoclimatic record provided by eolian deposition in the deep sea: the geologic history of wind. Rev Geophys 32(2):159–195. https://doi.org/10.1029/93RG03257
Rea DK, Janecek TR (1981) Mass-accumulation rates of the non-authigenic inorganic crystalline (Eolian) component of deep-sea sediments from the western mid-pacific mountains, deep sea drilling project site 463. In: Stout LN (ed) Initial reports of the deep sea drilling project volume 62. U.S. Government Printing Office, Washington, D.C., pp 653–659. https://doi.org/10.2973/dsdp.proc.62.125.1981
Singer A (1984) The paleoclimatic interpretation of clay minerals in sediments—a review. Earth Sci Rev 21(4):251–293. https://doi.org/10.1016/0012-8252(84)90055-2
Stewart RJ, Natland JH, Glassley WR (1973) Petrology of volcanic rocks recovered on DSDP leg 19 from the North Pacific Ocean and the Bering Sea. In: Initial Reports of the Deep Sea Drilling Project. U.S. Government Printing Office, Washington, D.C. https://doi.org/10.2973/dsdp.proc.19.114.1973
Stonecipher SA (1976) Origin, distribution and diagenesis of phillipsite and clinoptilolite in deep-sea sediments. Chem Geol 17:307–318. https://doi.org/10.1016/0009-2541(76)90044-9
Syers JK, Chapman SL, Jackson ML, Rex RW, Clayton RN (1968) Quartz isolation from rocks, sediments and soils for determination of oxygen isotopes composition. Geochim Cosmochim Acta 32(9):1022–1025. https://doi.org/10.1016/0016-7037(68)90067-7
Tanaka E, Nakamura K, Yasukawa K, Mimura K, Fujinaga K, Iijima K, Nozaki T, Kato Y (2020) Chemostratigraphy of deep-sea sediments in the western North Pacific Ocean: implications for genesis of mud highly enriched in rare-earth elements and yttrium. Ore Geol Rev 119:103392. https://doi.org/10.1016/j.oregeorev.2020.103392
Tanaka E, Nakamura K, Yasukawa K, Mimura K, Fujinaga K, Ohta J, Iijima K, Nozaki T, Machida S, Kato Y (2020b) Chemostratigraphic correlations of deep-sea sediments in the western North Pacific Ocean: a new constraint on the distribution of mud highly enriched in rare-earth elements. Minerals 10:575. https://doi.org/10.3390/min10060575
Tanaka E, Yasukawa K, Nakamura K, Ohta J, Miyazaki T, Vaglarov BS, Machida S, Fujinaga K, Iwamori H, Kato Y (2022) Secular variations in provenance of sedimentary components in the Western North Pacific ocean constrained by Sr isotopic features of deep-sea sediments. Geochem Geophys Geosyst 23:e2021GC009729. https://doi.org/10.1029/2021gc009729
Usui Y, Yamazaki T (2021) Magnetostratigraphic evidence for post-depositional distortion of osmium isotopic records in pelagic clay and its implications for mineral flux estimates. Earth Planets Space 73:2. https://doi.org/10.1186/s40623-020-01338-4
Usui Y, Shimono T, Yamazaki T (2018) Rock magnetism of quartz and feldspars chemically separated from pelagic red clay: a new approach to provenance study. Earth Planets Space 70:153. https://doi.org/10.1186/s40623-018-0918-1
Worden RH, Rushton JC (1992) Diagenetic K-feldspar textures: a TEM study and model for diagenetic feldspar growth. J Sediment Res 62:779–789. https://doi.org/10.1306/d42679d8-2b26-11d7-8648000102c1865d
Yamazaki T, Fu W, Shimono T, Usui Y (2020) Unmixing biogenic and terrigenous magnetic mineral components in red clay of the Pacific Ocean using principal component analyses of first-order reversal curve diagrams and paleoenvironmental implications. Earth Planets Space 72:120. https://doi.org/10.1186/s40623-020-01248-5
Ziegler CL, Murray RW (2007) Geochemical evolution of the central Pacific Ocean over the past 56 Myr. Paleoceanography 22(2):2203. https://doi.org/10.1029/2006pa001321
Ziegler CL, Murray RW, Hovan SA, Rea DK (2007) Resolving eolian, volcanogenic, and authigenic components in pelagic sediment from the Pacific Ocean. Earth Planet Sci Lett 254:416–432. https://doi.org/10.1016/j.epsl.2006.11.049

Publisher's Note

Springer Nature remains neutral with regard to jurisdictional claims in published maps and institutional affiliations.

Submit your manuscript to a SpringerOpen journal and benefit from:

- ► Convenient online submission
- ► Rigorous peer review
- ► Open access: articles freely available online
- ► High visibility within the field
- ► Retaining the copyright to your article

Submit your next manuscript at ► springeropen.com